PET Cardiac Imaging (Perfusion, Viability, Sarcoidosis, and Infection)

Padma Priya Manapragada, MD[a], Efstathia Andrikopoulou, MD[b], Navkaranbir Bajaj, MD[c], Pradeep Bhambhvani, MD[d,*]

KEYWORDS

• PET Cardiac • Perfusion • Viability • Sarcoidosis • Infection

KEY POINTS

- Access to novel radiopharmaceuticals and technological advances has led to the increased utilization of PET in cardiac perfusion and metabolic imaging resulting in improved diagnostic certainty and patient care.
- Assessment of myocardial perfusion with PET tracers enables not only high quality relative perfusion imaging but also allows for quantification of myocardial blood flow and flow reserve.
- PET myocardial viability imaging plays a significant role in risk stratifying patients with ischemic cardiomyopathy who may benefit from revascularization.
- FDG PET for sarcoidosis is valuable in diagnosis, estimating cardiac and extracardiac disease burden, treatment monitoring and prognosis.
- Reliable hot spot FDG PET in suspected cardiac inflammation or infection is possible only when physiologic myocardial FDG uptake is suppressed. Thus optimal patient preparation is crucial.

MYOCARDIAL PERFUSION USING POSITRON EMISSION TOMOGRAPHY

Coronary artery disease (CAD) continues to be the major cause of morbidity and mortality in both developing and developed countries.[1] The American Heart Association reports approximately 16 million people greater than or equal to 20 years old in the United States have cardiovascular disease.[2] CAD leads to approximately one-third of all deaths in people older than 35 years.[3] Understanding of CAD has improved significantly over the past several decades. PET using different flow tracers has led to translation of qualitative and quantitative estimation of myocardial blood flow (MBF) to clinical practice and research. The information derived during the cardiac PET scan can aid clinicians in phenotyping myocardial perfusion abnormalities and thus help treat their patients better. This section briefly discusses MBF anatomy and physiology to understand the role of myocardial perfusion PET imaging to determine alterations in this physiology. Technical considerations, current clinical indications, and applications also are discussed.

Myocardial Blood Flow: Anatomy and Physiology

The coronary arteries arise from the right and the left coronary sinuses/cusps of the aorta. The left coronary artery divides into left anterior descending and the left circumflex artery, whereas the right coronary artery travels in the right atrioventricular

The authors have nothing to disclose.
[a] University of Alabama at Birmingham, 619 19th Street South JT 772, Birmingham, AL 35249, USA; [b] University of Alabama at Birmingham, Tinsley Harrison Tower, Suite 311, 1900 University Boulevard, Birmingham, AL 35233, USA; [c] Asheville Cardiology Associates, 5 Vanderbilt Park Drive, Asheville, NC 28803, USA; [d] University of Alabama at Birmingham, 619 19th Street South JT 777, Birmingham, AL 35249, USA
* Corresponding author.
E-mail address: pbhambhvani@uabmc.edu

Radiol Clin N Am 59 (2021) 835–852
https://doi.org/10.1016/j.rcl.2021.05.009

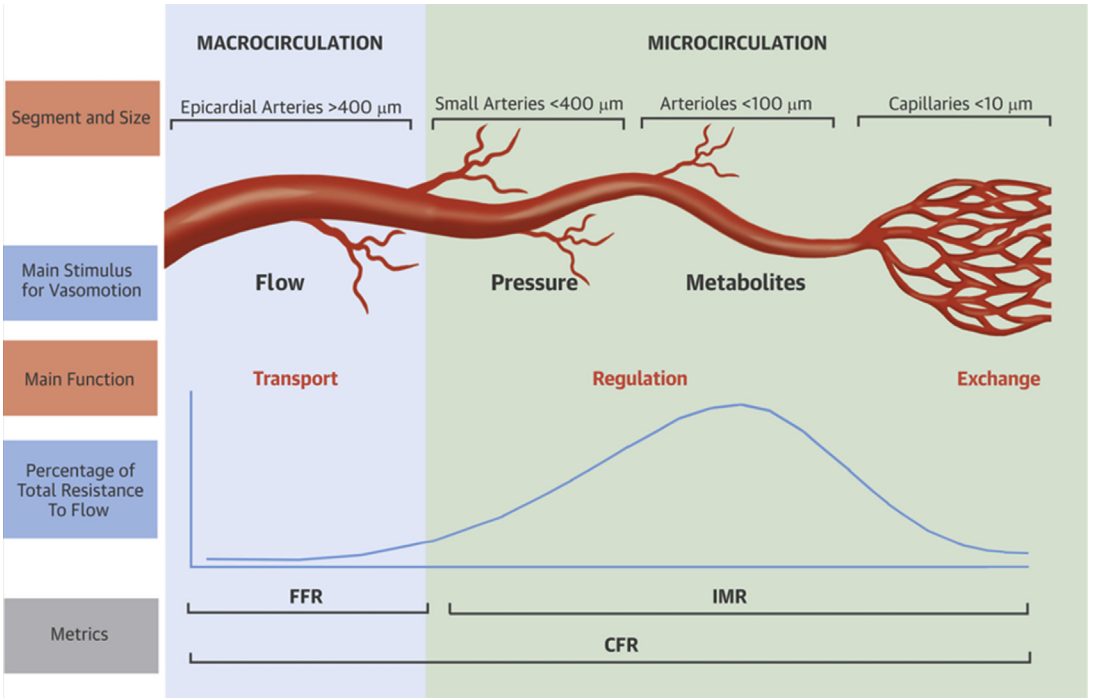

Fig. 1. Macrocirculation and microcirculation across segments and sizes of the arteries. FFR versus IMR versus CFR. (Adapted from De Bruyne B, Oldroyd KG, Pijls NHJ. Microvascular (Dys)Function and Clinical Outcome in Stable Coronary Disease. Journal of the American College of Cardiology. 2016;67(10):1170 to 1172.)

groove and commonly gives rise to posterior descending artery. These epicardial coronary arteries form the main branches of the coronary tree. These main coronary arteries then divide and subdivide into a filigree network of intramural coronary vessels, precapillary sphincters, capillaries, and coronary veins (**Fig. 1**). Different parts of coronary tree have different functions. For example, the epicardial coronary arteries contribute to the coronary capacitance, but, under most conditions, they have only a small effect on coronary vascular resistance. In contrast, the small transmural coronary vessels (<100 μm) play a dominant role in regulating total coronary vascular resistance. **Fig. 1** briefly describes the function of different segments of the coronary tree along with the commonly measured myocardial and coronary perfusion metrics, which aid in diagnosis of alterations MBF. Fractional flow reserve (FFR) measured during coronary angiography measures the transport function of epicardial coronary arteries and aids in the diagnosis of obstructive epicardial CAD, whereas index of microcirculatory resistance (IMR) measures coronary microvascular resistance; and coronary flow reserve (CFR) is a combined measure of abnormalities in the epicardial and microcirculation.[4]

Understanding Myocardial Blood Flow Physiology with Positron Emission Tomography

Myocardial perfusion imaging (MPI) with single-photon emission computed tomography (SPECT) is a widely used diagnostic and prognostic test for detection and risk stratification of patients with CAD. There is wealth of data supporting its use. MPI with SPECT and PET is limited by the relative nature of perfusion imaging, which may lead to difficulty in detection of global reduction in myocardial perfusion and thus underestimation of the extent of CAD. This fundamental limitation applies to MPI with both thallium-201–labeled and technetium-99m–labeled tracers.[5] With the use of PET, this issue with relative flow can be overcome due to better energy, spatial, temporal, and camera characteristics, allowing for global and regional MBF quantification in mL/min/g of tissue. Additional routine computed tomography (CT) attenuation correction with PET also leads to better-quality images with less artifacts.

Quantification of MBF using PET, allows assessment of peak hyperemic MBF as well as noninvasive calculation of CFR, a measure that evaluates the effects of abnormality over the entire coronary circulation (see **Fig. 1**). It, therefore, allows

assessment not only of the effects of focal epicardial coronary stenosis but also of diffuse coronary atherosclerosis and microvascular dysfunction. The use of CFR measured by PET has helped diagnose balanced ischemia, atherosclerosis, and microvascular dysfunction. The CFR also appears to be a very strong prognostic measure of adverse cardiovascular events even in those without obstructive epicardial CAD.[6–8]

Technical Considerations

Perfusion tracers

The blood flow tracers used most commonly are ^{82}Rb-chloride and ^{13}N-ammonia, with a small number of centers around the world using ^{15}O-water. ^{18}F-flurpiridaz, another perfusion tracer, currently is under investigation. Because of their short half-lives, ^{13}N-ammonia and ^{15}O-water require an on-site cyclotron and ^{82}Rb, a generator. In contrast, ^{18}F-flurpiridaz, because of its longer physical half-life (110 min), can be produced in batches and distributed regionally as is done with ^{18}F-fluorodeoxyglucose (FDG).

Scanner performance

Contemporary PET scanners operate in 3-dimensional (3-D) acquisition mode, as opposed to the older 2-dimensional (2-D) (or 2-D/3-D) systems that were constructed with interplane septa designed to reduce scatter. The 3-D systems generally require lower injected activity, with a concordant reduction in patient radiation effective dose.

Image acquisition and analysis

Image acquisition consists of relative static perfusion images, gated images, and list mode acquisition for estimation of MBF after stress and rest. Quantification of MBF requires accurate measurement of the total tracer activity transported by the arterial blood and delivered to the myocardium over time. Measurements of arterial isotope activity versus time (time–activity curves) typically are acquired using image regions of interest in the arterial blood pool (eg, left ventricle [LV], atrium, or aorta).[9,10]

Stress test procedure

In the United States, regadenoson is the agent utilized most commonly for inducing hyperemia through coronary vasodilation.[10] Other agents, adenosine and dipyridamole, also are used.[9,10] Exercise stress maybe performed but is technically challenging due to short half-lives of radiotracers, smaller bores of PET gantry for supine bicycles, and motion artifacts from exercising.

Patient preparation for pharmacologic stress with PET is the same as for ^{99m}Tc SPECT MPI.[10] Patients fast for a minimum of 4 hours, avoid smoking for at least 4 hours, and avoid caffeine intake for at least 12 hours before vasodilator stress. Rest imaging should be performed before stress. Vasodilator stress with the chosen agent is followed by radiotracer injection and imaging at stress. Rest and stress images usually are performed the same day. The dose of radiotracer depends on the type of PET camera and patient weight.[11]

Image acquisition and reconstruction parameters

Images are acquired and reconstructed using standard vendor-specific parameters. Briefly, after a low-dose CT or a radionuclide-localizing scan to position the heart, a dynamic or preferably list-mode acquisition is acquired in 2-D or 3-D mode. List-mode acquisition provides comprehensive data for static images, gated images for LV volumes and ejection fraction (EF), and dynamic images for MBF quantitation. The relative and quantitative perfusion images are reconstructed from CT attenuation-corrected images.[9,10]

Indications and applications

American Society of Nuclear Cardiology[10] recommends the use of PET over SPECT myocardial perfusion when 1) Prior stress imaging study was of poor quality, equivocal or inconclusive 2) Body characteristics that commonly affect image quality. Some examples include large breasts, breast implants, obesity (BMI greater than 30), protuberant abdomen, chest wall deformities, pleural effusions, and inability for proper body positioning such as inability to position arms outside of a SPECT scanner's field of view 3) High-risk patients in whom diagnostic errors carry even greater clinical implications. Some examples include chronic kidney disease stages 3, 4 or 5; diabetes mellitus; known or suspected potentially high-risk CAD such as left main, multivessel, or proximal LAD disease or extensive coronary disease. 4) Young patients with established CAD who are anticipated to need repeated exposures to radiation-associated cardiac imaging procedures. 5) Patients in whom myocardial blood flow quantification is a needed adjunct to the imaging findings. Several investigational uses of myocardial perfusion imaging are also on the cusp of translation into clinical medicine including those suspected to have microvascular disease, cardiometabolic risk factors including those with obesity, CKD, and diabetes, heart transplant, and infiltrative cardiomyopathies.

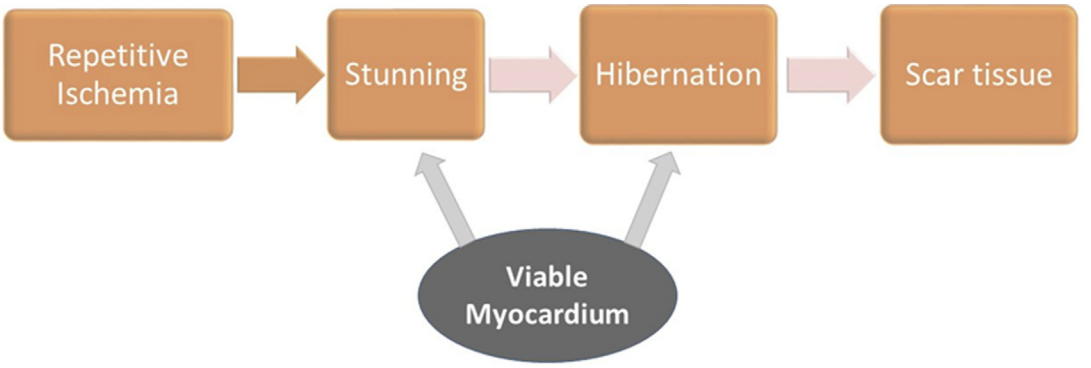

Fig. 2. Continuum of dysfunctional myocardium with subcategories of viable myocardium, that is, stunning and hibernation. Repetitive episodes of hypoperfusion and ischemia cause the development of stunned myocardium. Stunning denotes abnormal myocardial contractility in the presence of normal resting blood flow. Recurrent episodes of stunning in turn lead to hibernating myocardium, which is characterized by reduced resting blood flow and certain ultrastructural cardiomyocyte alterations, namely increased glycogen plaques and loss of their sarcoplasmic reticulum, T tubules, and contractile apparatus. Irrespective of the presence of normal or reduced resting blood flow (stunning vs hibernation), CFR is diminished, which in turn results in demand ischemia. Stunned and hibernating myocardium both are salvageable or viable, meaning that restoration of coronary perfusion may result in recovery of normal function/contractility. If no intervention is undertaken, however, to restore perfusion, hibernating myocardium evolves into scar tissue (irreversibly necrotic myocardium), characterized by alterations in gene expression, loss of mitochondrial function, increase in the myocardial extracellular space, and myocardial fibrosis. Scarred myocardium is seen as irreversibly adverse LV remodeling on cardiac imaging (echocardiography, CMR, and cardiac CT). Both scarred and hibernating myocardium may serve as substrates for ventricular arrhythmias and may increase the risk for sudden cardiac death.

PET VIABILITY

Background

Despite the advances in diagnosis, imaging, medical management, and revascularization techniques, one-third of patients following an acute myocardial infarction develop ischemic heart failure (ischemic cardiomyopathy [ICM]).[12] In 2010, the prevalence rates of ICM were 190 per 100,000 person-years and 270 per 100,000 person-years in women and men, respectively, and these rates are only expected to rise as the population ages and survival improves.[13] Viability imaging plays a significant role in risk stratifying patients with ICM who may benefit from revascularization. From an ultrastructural standpoint, viability refers to the preservation of contractile function based on cellular, metabolic, and microscopic characteristics. Clinically, the presence of viable myocardium denotes dysfunctional myocardium at rest, which may recover part or all of its contractile function following restoration of coronary perfusion.

There are 2 main categories of viable myocardium, namely hibernation and stunning, which fall on a continuum of abnormalities in myocardial perfusion and function (**Fig. 2**). Myocardial stunning results from transient, repetitive episodes of hypoperfusion and is characterized by reduced contractile function in the presence of normal resting blood flow. Recurrent episodes of stunning over time eventually leads to the development of hibernating myocardium characterized by reduced resting blood flow and associated alterations both at the ultrastructural cardiomyocyte level and at the macroscopic, LV level. From a macroscopic standpoint, hibernation manifests as adverse LV remodeling, LV dilation, and LV systolic and

Table 1
Differences between myocardial stunning and hibernation

Features	Stunning	Hibernation
Reduced flow at rest	×	✓
Abnormal contractile function	✓	✓
Reduced CFR	✓	✓
Histopathologic abnormalities	✓	✓
Potential for recovery of LV function following revascularization	✓	✓
May progress to	Hibernation	Scar

Abbreviations: ×, Absent; ✓, Present.

diastolic dysfunction. The main distinguishing characteristics of stunning and hibernation are listed in **Table 1**. These can be visualized by echocardiography, cardiac magnetic resonance (CMR), and cardiac CT. Myocardial radionuclide imaging, including SPECT and PET, rely on detecting changes in coronary perfusion and cardiomyocyte metabolism. Compared with SPECT, PET offers higher spatial and energy resolution and lower radiation exposure. These advantages are crucial when assessing for LV viability, when detection of scar versus hibernation is critical. The focus of this section is on providing an overview of FDG PET imaging for the evaluation of myocardial viability.

Protocols for Imaging

Normal myocardium utilizes long-chain fatty acids as its primary source of energy; however, under anaerobic conditions, for example, coronary hypoperfusion and ischemia, cardiomyocytes switch to glucose as their main energy source. The process of glucose uptake by the cardiomyocytes is active and mediated by insulin secretion. Appropriate management of glucose and insulin levels is key for generating diagnostically accurate and high-quality myocardial FDG PET studies for assessment of viability.

Evaluation of coronary perfusion and myocardial metabolism are the 2 key components of viability examination. Perfusion imaging can be performed either by SPECT tracers or by PET tracers, which are surrogates for the integrity of cardiomyocyte cellular membrane. Perfusion imaging at rest should be performed first; if there are no perfusion defects, this means that all LV segments are viable and evaluation for myocardial ischemia may be considered. If, however, there are resting perfusion defects, viability metabolic imaging can be undertaken with FDG.

The importance of patient preparation should be emphasized to provide examinations of high diagnostic quality. Following a 6-hour to 12-hour fast, plasma glucose is checked. Depending on this initial value, patients are administered an oral glucose load (25–100 mg), which leads to a transient increase in plasma glucose, stimulates pancreatic insulin secretion, and ultimately shifts myocardial consumption from fatty acids to glucose. Following the oral glucose load, intravenous insulin is administered to achieve euglycemic state prior to FDG injection.[11] An alternative to glucose loading is acipimox, a nicotinic acid derivative approved for use in Europe, which functions by inhibiting peripheral lipolysis, reducing levels of free fatty acids (FFAs), and ultimately increasing levels of glucose. Another alternative technique is the euglycemic-hyperinsulinemic clamp, which is a rigorous and time-consuming procedure.[11] The target range for plasma glucose prior to administering FDG is 100 mg/dL to 140 mg/dL. Once glucose is within this range, FDG is injected and the patient is monitored for 45 minutes to 90 minutes prior to undergoing PET imaging. To ensure patient safety, glucose levels are monitored after FDG injection. Typically, 5 mCi to 15 mCi (185–555 MBq) of FDG is administered and image acquisition usually lasts 10 minutes to 30 minutes. An overview of the protocol is shown in **Fig. 3**.

Once both perfusion and metabolism imaging are completed, the 2 image data sets are aligned, and interpretation is based on 1 of the 4 distinct perfusion-metabolism patterns, as shown in **Fig. 4**. There are certain limitations of FDG viability assessment, namely FDG uptake, that can be impacted by the degree of underlying ischemia, coexisting abnormalities in sympathetic activity, and the severity of reduction in cardiac output/severity of underlying heart failure.[14]

Clinical Implications and Value of PET Viability Assessment

The results from multiple, single-center, observational, nonrandomized studies have shown viability imaging to be valuable in guiding decision making regarding revascularization in patients with ICM, meaning that patients with hibernating (viable) myocardium have been found to have lower mortality following revascularization. Di Carli and colleagues showed that in patients with viable myocardium detected by PET imaging, surgical revascularization compared with medical management was associated with improved 4-year survival (75% vs 30%; $P = .007$) as well as improvement in the severity of angina and symptoms of heart failure.[15–17] A more recent study on 648 patients by Ling and colleagues[18] also found that revascularization correlated with improved survival in patients with hibernating myocardium, particularly in those with more than 10% viable myocardium. These findings highlight one of the important criteria in assessing the benefits of revascularization in patients with hibernating myocardium, namely the extent of viability/hibernation. It has been shown that in patients with a higher mismatch of perfusion-metabolism (ie, larger extent of hibernation), the benefits from revascularization are larger.[19] The opposite also is true, meaning when the extent of mismatch is small (less than 7%), there is not much value in pursuing revascularization. Additional factors that should be considered when planning for

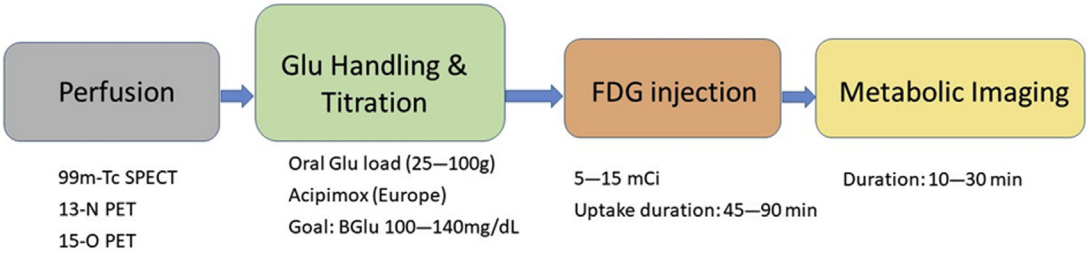

Fig. 3. Imaging protocol for ^{18}F-FDG PET viability assessment. Following administration of the perfusion tracer, perfusion imaging is performed either by means of SPECT or PET MPI. In the United States, ^{13}N-ammonia and ^{82}rubidium are clinically available PET tracers whereas in Europe both ^{13}N-ammonia and ^{15}O-water are available. Handling and titration of plasma glucose follow acquisition of perfusion image data set. The patient's baseline blood glucose is checked and, if less than 250 mg/dL, an oral glucose load is administered. Levels of blood glucose are checked frequently (every 10–15 min) and intravenous insulin is administered based on predefined protocols, to achieve a target plasma glucose of 100 mg/dL to 140 mg/dL. The goal is to shift myocardial energy consumption from fatty acid to glucose. Acipimox is a nicotinic acid derivative, which is an alternative to oral glucose loading. Once the plasma glucose is within the goal range of 100 mg/dL to 140 mg/dL, FDG is injected (5–15 mCi [185–555 MBq]). The patient then is monitored for 45 minutes to 90 minutes (uptake phase), during which time, blood pool concentrations of FDG decrease whereas myocardial FDG uptake increases. A higher signal-to-noise ratio can be achieved by waiting for the full 90 minutes, because blood pool FDG levels re very low while myocardial levels continue to rise. This can be beneficial particularly in diabetic patients, who pose a particular challenge due to high insulin resistance and high basal insulin requirements. Metabolic imaging is performed, which usually takes 10 minutes to 30 minutes to complete. The perfusion and metabolic image datasets then are aligned and evaluation for perfusion-metabolism patterns performed to allow for identification of viable (hibernating) myocardium versus scar versus stunning versus normal.

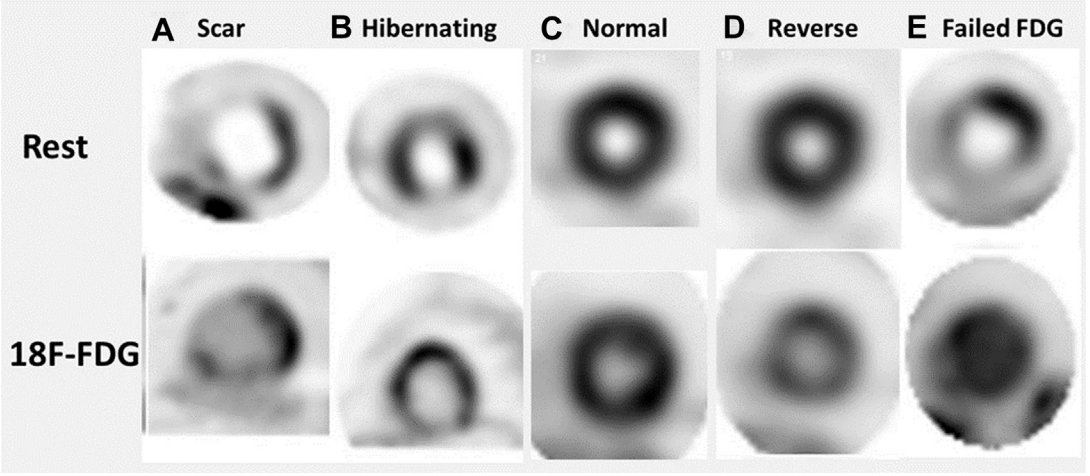

Fig. 4. Four patterns of perfusion-metabolism. (*A*) Matched perfusion and metabolism, where both are abnormal. The presence of a resting perfusion defect with accompanying defect on FDG metabolic imaging signifies absence of viability and presence of scared myocardium. There is a low likelihood this patient will experience improvement in LV dysfunction and adverse remodeling following revascularization. (*B*) Perfusion-metabolism mismatch involving the anterior wall, where a resting perfusion defect is accompanied by normal FDG uptake. This signifies the presence of viable, hibernating myocardium in the anterior wall. This patient has a high likelihood of experiencing improvement in LV systolic function and adverse remodeling following revascularization. Also note the presence of a matched perfusion-metabolism defect involving the inferior wall, which denotes scar. (*C*) Matched perfusion and metabolism where both are normal. This denotes normal myocardium at rest. If the patient experiences chest pain, angina, or other symptoms suggestive of ischemia, ischemia assessment should be considered. (*D*) Perfusion-metabolism mismatch, where there is no resting perfusion defect, but there is accompanying reduction in FDG uptake. This usually is seen in patients with left bundle branch block as a mismatch in the interventricular septum and also has been described in patients with stunning or significant insulin resistance. (*E*) Example of patient with high insulin resistance and poorly controlled diabetes mellitus resulting in poor-quality FDG images precluding accurate viability assessment.

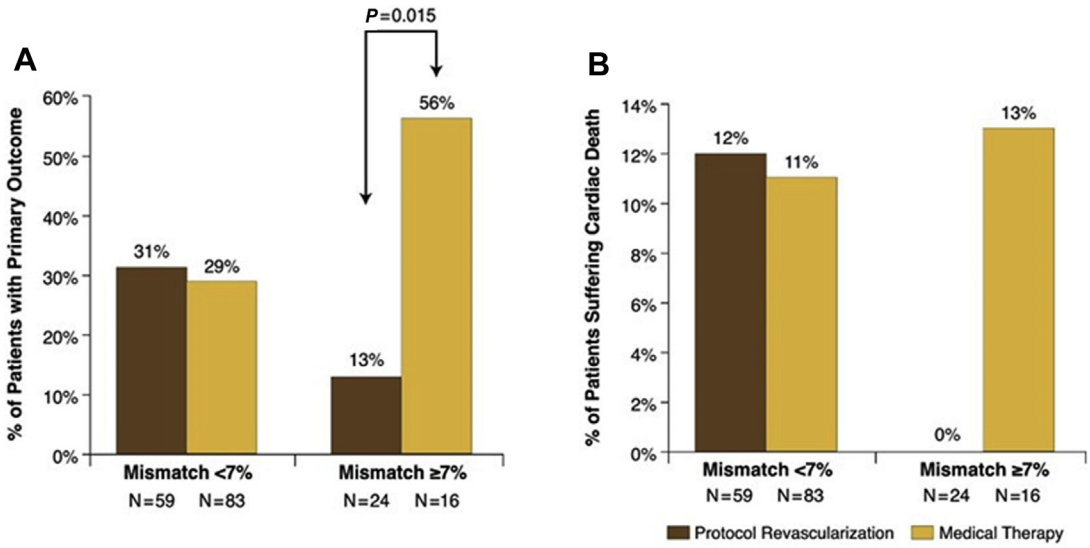

Fig. 5. (*A*) Proportion of patients who were randomized to either FDG-guided revascularization or medical therapy based on standard of care and who experienced the composite outcome of cardiac death, myocardial infarction, hospitalization due to unstable angina or heart failure, or heart transplantation within 1 year. The results are classified based on the size of perfusion-metabolism mismatch using 7% as the cutoff. In the subgroup with mismatch of less than 7%, revascularization was not associated with a significant improvement in the primary outcome compared with medical treatment (P = .923). In contrast, in the subgroup with mismatch greater than or equal to 7%, revascularization correlated with lower rates of the primary composite endpoint (P = .015). (*B*) Proportion of patients who were randomized to either FDG-guided revascularization or medical therapy based on standard of care and who experienced cardiac death within 1 year. In the subset of patients with mismatch less than 7%, revascularization was not associated with a significant difference in cardiac mortality. No cardiac deaths were noted in the subset of patients with mismatch greater than or equal to 7% who underwent FDG guided revascularization compared with 2 patients (15%) who were treated medically. (Adopted with permission from D'Egidio G, Nichol G, Williams KA, et al. JACC Cardiovasc Imaging 2009; 2:1060–1068.)

revascularization include the LVEF and the renal function.[20] Despite showing benefit of PET viability imaging to guide revascularization, these studies have undergone scrutiny due to their nonrandomized, single-center, observational design and due to the potential for including confounders and some of them only having small number of hard outcomes.[21,22]

To date the PET and Recovery Following Revascularization-2 (PARR 2) has been the only large, multicenter study that randomized 430 patients with known or suspected CAD to either FDG PET/CT viability imaging versus standard of care.[23] Over a 12-month follow-up, patients who underwent PET viability imaging showed a nonsignificant lower composite outcome of cardiac mortality, myocardial infarction, or hospitalization due to heart failure or angina.[23] In contrast, a post hoc analysis of 5-year follow-up comparing patients who adhered to PET recommendations for revascularization versus standard of care showed a significant improvement in event-free survival in the former and in those patients with a mismatch of at least 7% in extent (**Fig. 5**).[24,25] Two important caveats of the PARR 2 are that only 25% of patients adhered to the PET-guided recommendations for revascularization and the variability in PET-related resources and expertise, which may have influenced decision making and patient management.[19,25] Future research for evaluation of the advantage of using advanced imaging (PET and CMR) is the focus of Alternative Imaging Modalities in Ischemic Heart Failure (AIMI-HF) trial, which itself is part of the larger, multitrial project of Imaging Modalities to Assist with Guiding Therapy and the Evaluation of Patients with Heart Failure (**Fig. 6**).[26]

When to Perform PET Viability Assessment

According to the most recent guidelines published by the American College of Cardiology and the American Heart Association, viability assessment using imaging is reasonable in patients with new-onset heart failure without angina and with known underlying significant CAD, provided the patient is an eligible candidate for revascularization (class IIa, level of evidence C).[27] The appropriate use criteria also are in accordance with this grading,

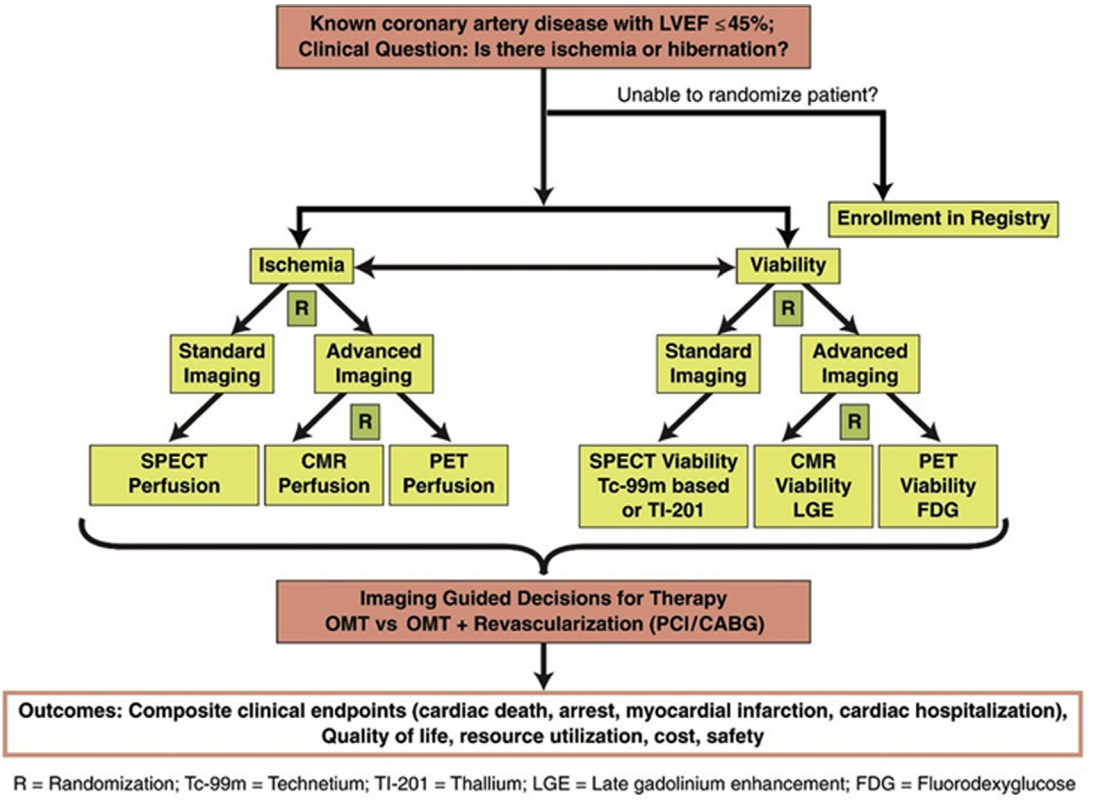

Fig. 6. Study design of the AIMI-HF trial, is a combined randomized and registry study. Participants will be randomized either to advanced or standard imaging, depending on whether the primary clinical concern is the presence of ischemia versus viability. Patients not eligible for randomization will be assigned to a clinical registry. The primary outcome is a composite endpoint of cardiac mortality, cardiac hospitalization, myocardial infarction, or resuscitated cardiac arrest. (Adapted with permission from Mielniczuk LM, Toth GG, Xie JX et al. JACC Cardiovasc Imaging. 2017;10(3):354-64.)

that is, noninvasive imaging for viability assessment is appropriate or "may be appropriate" in most cases of LV systolic dysfunction (**Table 2**).[28] The most recent scientific statement from the American Heart Association on viability imaging provides algorithms for noninvasive imaging with CMR and FDG PET in patients with chronic and subacute ischemic LV systolic dysfunction.[29]

Conclusion

Noninvasive myocardial viability assessment using FDG PET so far has proved beneficial in prognosticating patients who may benefit from improved LV systolic function, quality of life, and survival following revascularization. Additional larger, randomized, multicenter studies are needed to better define the PET criteria that can be used to predict outcomes following revascularization. A heart team approach comprising cardiologists, surgeons, and imagers should be implemented to provide each patient with personalized recommendations by integrating clinical, imaging and laboratory data.

PET FOR SARCOIDOSIS

Sarcoidosis is an immune-mediated systemic disease of unknown etiology, characterized by granulomatous inflammation of various organs.[30] Sarcoidosis first was described in 1877 by the dermatologist Jonathan Hutchinson, who described violaceous skin lesions.[31] Sarcoidosis diagnosis is made based on history, physical examination, appropriate radiologic and pathologic findings, and exclusion of other causes.[32]

Cardiac involvement often occurs with sarcoidosis (cardiac sarcoidosis [CS]); however, it produces symptoms in approximately only 5% of patients.[33] The prevalence of CS in the United States is approximately 25% for patients with sarcoidosis.[34] Clinical manifestations of CS are quite variable and range from a lack of any clinical symptoms to sudden death. Other presentations

Table 2
Indications for use of PET viability imaging in the 2013 appropriate use criteria

PET Viability Imaging in Patients Eligible for Revascularization	Rest Imaging	Stress/Rest Imaging
Severe LV systolic dysfunction (LVEF< 30%)	Appropriate	Appropriate
Moderate LV systolic dysfunction (LVEF: 30%–39%)	Appropriate	May be appropriate
Mild LV systolic dysfunction (LVEF: 40%–49%)	May be appropriate	Appropriate

Adapted from Patel MR, White RD, Abbara S, et al. 2013 ACCF/ACR/ASE/ASNC/SCCT/SCMR appropriate utilization of cardiovascular imaging in heart failure: a joint report of the American College of Radiology Appropriateness Criteria Committee and the American College of Cardiology Foundation Appropriate Use Criteria Task Force. J Am Coll Cardiol. 2013;61(21):2207-2231.

include dizziness, palpitations, syncope or near syncope, dyspnea, orthopnea, peripheral edema, chest pain, conduction abnormalities, and cardiac failure. Inflammatory granulomas or postinflammatory scarring may lead to conduction abnormalities, arrhythmias, sudden cardiac death, and congestive heart failure.[35] The myocardium is the region affected most frequently, especially the ventricular septum and LV free wall. Sarcoidosis also can involve the coronary arteries, pericardium, and valves.[34,36]

Isolated CS (ICS) is a distinct clinical phenotype. Established criteria for the diagnosis of CS are insensitive for ICS because they require either evidence of extracardiac disease or a positive endomyocardial biopsy (EMB). EMB is highly limited in its sensitivity of approximately 20% to 30%, because it often misses areas of patchy myocardial involvement.[37] As many as 25% of patients with CS may have ICS. Patients with ICS have worse LV systolic function and event-free survival and more ventricular arrhythmias compared with patients with systemic sarcoidosis and CS.[38]

Because of the potential life-threatening complications and potential benefit of treatment, all patients diagnosed with sarcoidosis should be screened for cardiac involvement. CMR and FDG PET/CT have nearly replaced other imaging techniques due to their higher accuracy for diagnosing CS.[35] PET/CT has been included in the diagnostic algorithm for CS by the Heart Rhythm Society in 2014[39] and the revised Japanese Society of Cardiac Sarcoidosis in 2017.[40]

A joint expert consensus document of the Society of Nuclear Medicine and Molecular Imaging (SNMMI) and ASNC by Chareonthaitawee and colleagues recommend PET/CT for the assessment of CS in (1) patients with histologic evidence of extra CS and 1 or more abnormal screening results for CS, (2) new-onset sustained second-degree or third degree atrioventricular block and age less than 60 years, (3) idiopathic sustained ventricular tachycardia, and (4) serial studies to assess response to treatment.[41,42]

Optimal patient preparation is essential when using FDG PET/CT to evaluate CS. It is imperative that physiologic myocardial uptake FDG be suppressed to identify areas of pathologic involvement. Standardized guidelines developed by SNMMI and ASNC recommend at least 2 high-fat (>35 g) and low-carbohydrate (<3 g) meals the day prior to the FDG PET/CT, followed by a fast of 4 hours to 12 hours prior to the study. An alternative option (for patients who cannot follow the diet) is fasting for greater than of equal to 18 h before the study.[42,43]

All CS patients scheduled for FDG PET should undergo rest MPI to compare perfusion images

Table 3
Classification of cardiac sarcoidosis stage based on perfusion and metabolism pattern

Disease Stage	Perfusion and Metabolism Pattern
Stage 1	Normal perfusion and no FDG uptake
Stage 2: mild or early disease	Patchy FDG uptake in an area with normal or only mildly decreased perfusion
Stage 3: moderate or progressive disease	FDG uptake in an area with a corresponding moderate perfusion defect
Stage 4: severe or fibrous disease	Severe perfusion defect but no or minimal corresponding FDG uptake

Data from Bokhari S, Lin JC, Julien HM. FDG-PET is a superior tool in the diagnosis and management of cardiac sarcoidosis https://www.acc.org/latest-in-cardiology/articles/2017/04/10/08/43/fdg-pet-is-a-superior-tool. Published April 10, 2017.

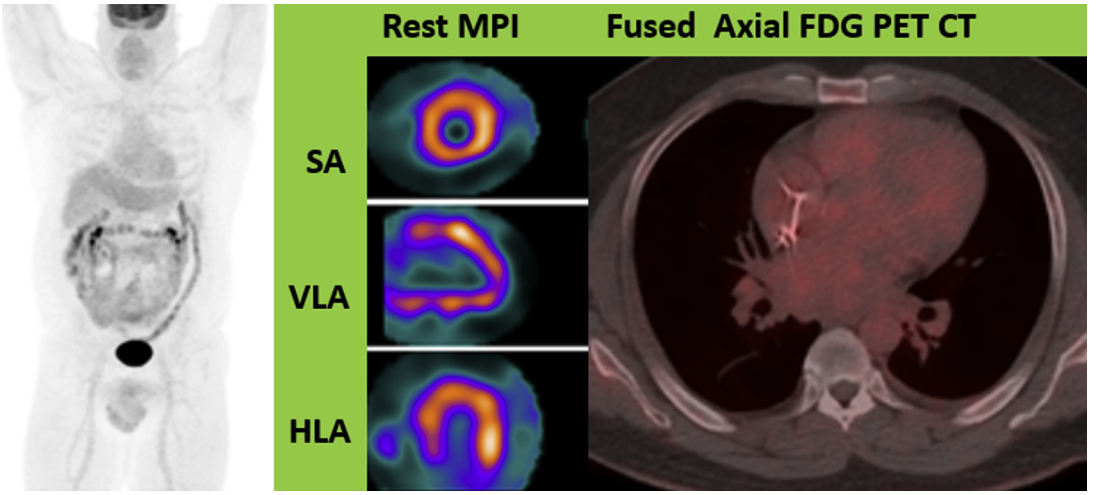

Fig. 7. A 49-year-old man with sarcoidosis and complete heart block, post-pacemaker placement, on immunosuppressive treatment. Stage 1 CS with normal Technetium-99m (99mTc) rest myocardial perfusion (*center panel*) and no active cardiac or extracardiac inflammation on MIP (*left panel*) and fused FDG PET/CT images (*right panel*). SA: Short Axis, VLA: vertical Long Axis, HLA: horizontal long axis.

with FDG PET images. After perfusion imaging, approximately 10 mCi (370 MBq) of FDG is injected intravenously to perform dedicated cardiac and optional whole-body FDG PET/CT scans. CS is categorized into stage I to stage IV, based on perfusion and metabolism patterns (**Table 3**). Rest perfusion images are classified as normal or abnormal. Regional myocardial perfusion is categorized further as normal (**Figs. 7 and 8**) or mildly, moderately, or severely reduced.[44] A resting myocardial perfusion defect in these patients could be attributed to microvascular compression from inflammation or may be due to scar. FDG images are considered normal when there is no myocardial FDG uptake (see **Fig. 7**). If concurrent FDG is noted in the same territory, then the perfusion defect likely is secondary to inflammation (**Fig. 9**). Myocardial scar is favored if FDG uptake is lacking in this territory with associated regional wall motion abnormality. Comparison of rest myocardial perfusion and FDG PET is essential to identify disease patterns (no inflammation, active inflammation, and scarring) and to evaluate response to therapy.[45]

FDG images are considered abnormal when there is a focal, heterogeneous, or focal on diffuse

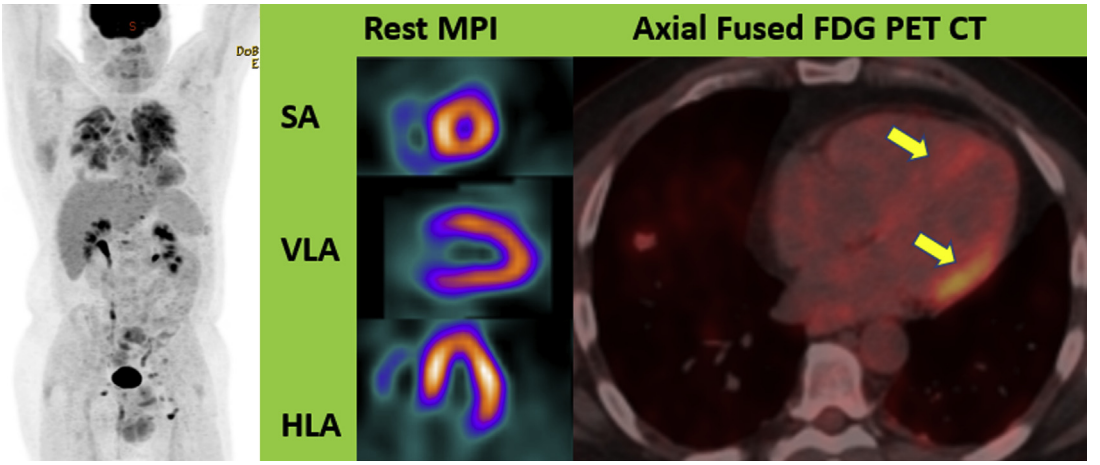

Fig. 8. A 57-year-old man with systemic sarcoidosis and right bundle-branch block. Rest perfusion is normal. FDG PET MIP shows extensive active pulmonary disease and hypermetabolic lymph nodes. Fused PET/CT images show active bilateral lung inflammation and patchy areas of FDG uptake involving the septal, anterior, and lateral myocardium, (*arrows*) from early myocardial sarcoid involvement (stage 2).

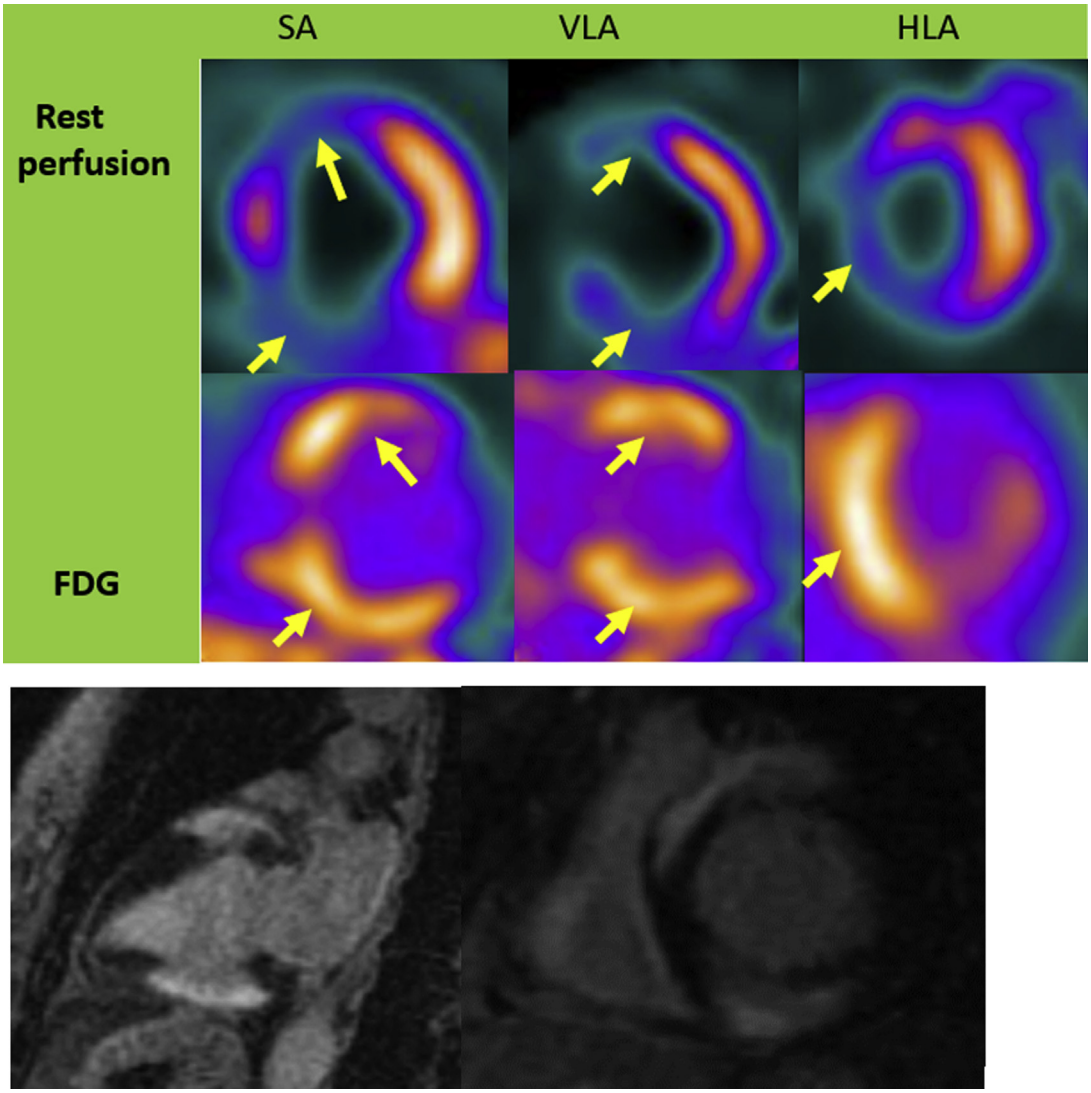

Fig. 9. A 62 -year-old woman with history of cardiac arrest. Rest perfusion images show decreased to absent basal to midanterior, anteroseptal, inferior, and inferoseptal myocardium, with corresponding FDG uptake (*arrows*)—moderate/progressive disease (stage 3). No extracardiac inflammation was identified, suggestive of ICS. CMR 2-chamber and short-axis images show subepicardial and midmyocardial late gadolinium enhancement along the anterior and inferior walls of LV, consistent with CS. HLA, horizontal long axis; SA, short axis; VLA, vertical long axis.

myocardial FDG uptake.[46] PET also helps in assessment of disease activity visually and with semiquantitative standardized uptake value (SUV) and in monitoring treatment response (**Fig. 10**); however, there is no specific SUV threshold that can be used to reliably delineate inflamed from normal myocardial tissue.[41] Whole-body FDG PET also is useful to evaluate the extent of systemic disease (see **Fig. 8**). FDG PET/CT is preferred in patients where CMR is contraindicated, in patients with implantable metallic devices (see **Fig. 10**), and in impaired renal function.[36] Blankstein and colleagues[46] have demonstrated the relationship between FDG uptake and focal perfusion defects, as shown by cardiac PET for identifying patients who are at higher risk of lethal arrhythmias and death.

Gallium-68 (^{68}Ga) DOTATATE, a somatostatin receptor–targeted radiotracer, is a potential alternative to FDG in imaging the CS patient. It is a commonly used tracer in neuroendocrine tumor imaging. ^{68}Ga-DOTATATE also targets activated

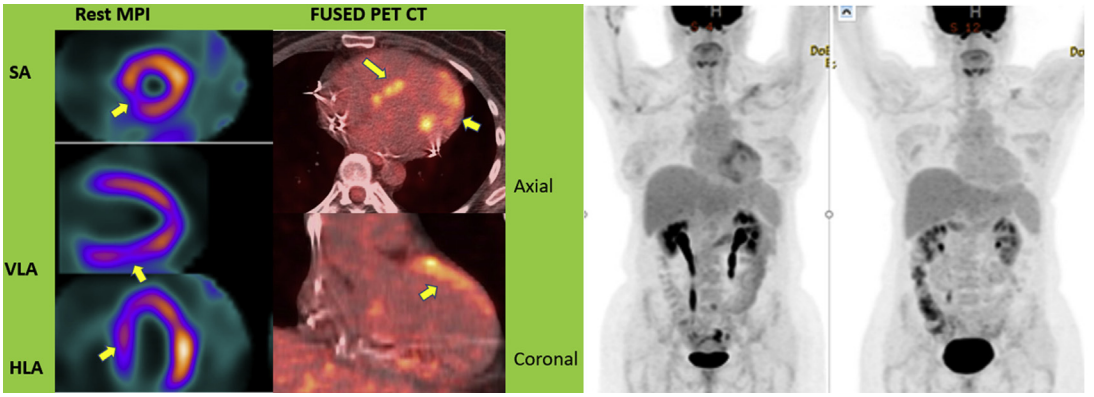

Fig. 10. A 54-year-old woman with CS. Rest perfusion images with abnormal perfusion in septum and inferior wall (*arrows*, left/1st column). Fused FDG PET-CT and MIP images with focal on diffuse uptake, notable in the anterior, inferior, anterolateral, and septal myocardium, consistent with active inflammation (2nd and 3rd column). Follow-up PET CT showing significant improvement after patient placed on steroids and immunosuppression, as shown on MIP images (right/4th column). This patient could not undergo CMR due to an incompatible defibrillator. HLA, horizontal long axis; SA, short axis; VLA, vertical long axis.

macrophages and multinucleated cells, which express somatostatin receptors. It does not target normal myocardial tissue, which lacks somatostatin receptors, and therefore possibly is suitable for patients with limitations to the adherence of FDG myocardial suppression protocols. ^{68}Ga-DOTATATE has a role in evaluating disease extent of sarcoidosis and can be used as guidance to different therapeutic options or prognosis, as proposed by Vachatimanont and colleagues.[47]

Integrated PET/MR imaging is promising. The integration of the metabolic PET imaging along with the morphologic, functional, and tissue imaging characteristics of MR imaging would improve diagnostic accuracy and potentially provide further prognostic and therapeutic insight in CS patients.[48] Wicks and colleagues[49] showed that hybrid PET/MR imaging was superior for detecting CS with sensitivity, specificity, positive, and negative predictive values of 0.94, 0.44, 0.76, and 0.80, respectively and abnormalities found on both PET and MR imaging was the strongest predictor of major adverse cardiac events.

Corticosteroid therapy is the first-line treatment of CS to reduce inflammation and prevent progression to fibrosis.[50] Starting therapy before LV dysfunction results in an excellent clinical outcome and is the mainstay in the treatment of CS. When CS patients present with sustained ventricular arrhythmias, use of implantable cardioverter-defibrillators (ICDs) is crucial.[51] Pacemaker implantation is recommended in patients with a high-grade or complete atrioventricular block.[52] Immunosuppressive therapies have been used in patients refractory to corticosteroids or in those who cannot tolerate their side effects. Treatment with methotrexate, azathioprine, or cyclophosphamide also is used as a steroid-sparing agent. In patients for whom corticosteroids are contraindicated, immunosuppressive agents are chosen for the initial treatment.[53] Orthotopic heart transplant is used increasingly for end-stage heart failure due to CS.[54]

^{18}F-FLUORODEOXYGLUCOSE PET IMAGING OF CARDIAC AND CARDIAC DEVICE INFECTIONS

Early and accurate diagnosis of cardiac valve and cardiac device infection is crucial for clinical decision making because these infections are associated with significant morbidity and mortality, especially when there is a delay in diagnosis and treatment. Cardiac implantable electronic devices (CIEDs) include pacemakers, ICDs, and cardiac resynchronization therapy devices with or without defibrillator. Cardiac device infections can be pocket and/or systemic infection. Pocket infection involves the subcutaneous pocket containing the generator and the subcutaneous portion of the leads. Systemic infection involves the transvenous segment of the lead (**Fig. 11**) or an epicardial electrode. Infection rates are lowest during initial implantation and 1.5-fold to 3-fold higher during revision or replacement.[55]

Diagnosis of cardiac and cardiac device infection is based on clinical manifestations, blood cultures (and other microbiologic data), and first-line

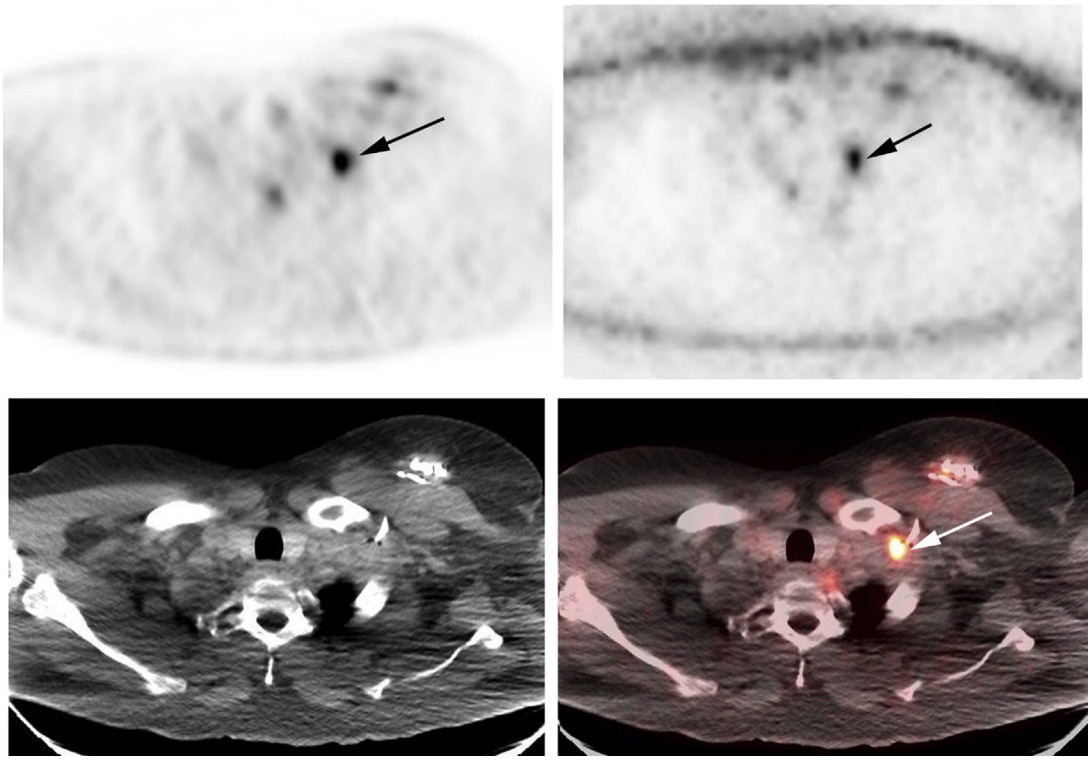

Fig. 11. Attenuation-corrected (*top left*), non-attenuation-corrected (*top right*), CT (*bottom left*), and fused PET/CT images (bottom right) show prominent focal hypermetabolic activity associated with left chest wall ICD lead infection (*arrows*) in the subclavian vein with tiny air bubbles in a patient with methicillin-sensitive Staphylococcus aureus bacteremia.

imaging with echocardiography. Although the utility of FDG PET for diagnosis of native valve infective endocarditis is limited, it is more useful for evaluating prosthetic valve endocarditis (**Fig. 12**). FDG PET not only promptly identifies the presence and extent of cardiac infection (abscess and paravalvular spread) but also demonstrates any embolic extracardiac infection (given the wide field of view) and primary source of infection, which can affect treatment decision making. In 1 study, extracardiac infection PET findings led to treatment change in 35% of patients.[56] Recent meta-analyses report a pooled sensitivity of 61% to 81% and pooled specificity of 78% to 88% for FDG PET diagnosis of infective endocarditis, with higher sensitivity for prosthetic valve endocarditis.[57,58] The pooled sensitivity and specificity of PET/CT diagnosis of CIED infection were 83% and 89%, respectively, with diagnostic performance of pocket infection better than lead infection.[59] FDG PET/CT also has high diagnostic accuracy for LV assist device infections, with pooled sensitivity of 92% and specificity of 83%.[60] Prognostically, an abnormal FDG PET is associated with greater major adverse cardiac events in prosthetic valve endocarditis.[61] Diemberger and colleagues[62] noted increased mortality in patients with FDG PET CIED lead infection but no pocket infection. FDG PET/CT has made it into guideline recommendations for diagnosis of infective endocarditis and cardiac device infection, with FDG avidity of a greater than 3-month-old prosthetic valve a major diagnostic criterion of infection.[63,64]

Increased glucose metabolism from increased glucose transporter-1 expression to meet the higher energy demands of activated inflammatory cells (leukocytes and macrophages) is the basis of FDG PET infection and inflammation imaging.[65] Reliable hot spot FDG PET in suspected cardiac infection is possible only when physiologic myocardial FDG uptake is suppressed. The heart uses various substrates for its energy needs, including FFAs, glucose, and lactate. Thus, interventions that facilitate myocardial FFA metabolism while simultaneously suppressing physiologic glucose metabolism are imperative for successful FDG PET cardiac infection imaging.[66]

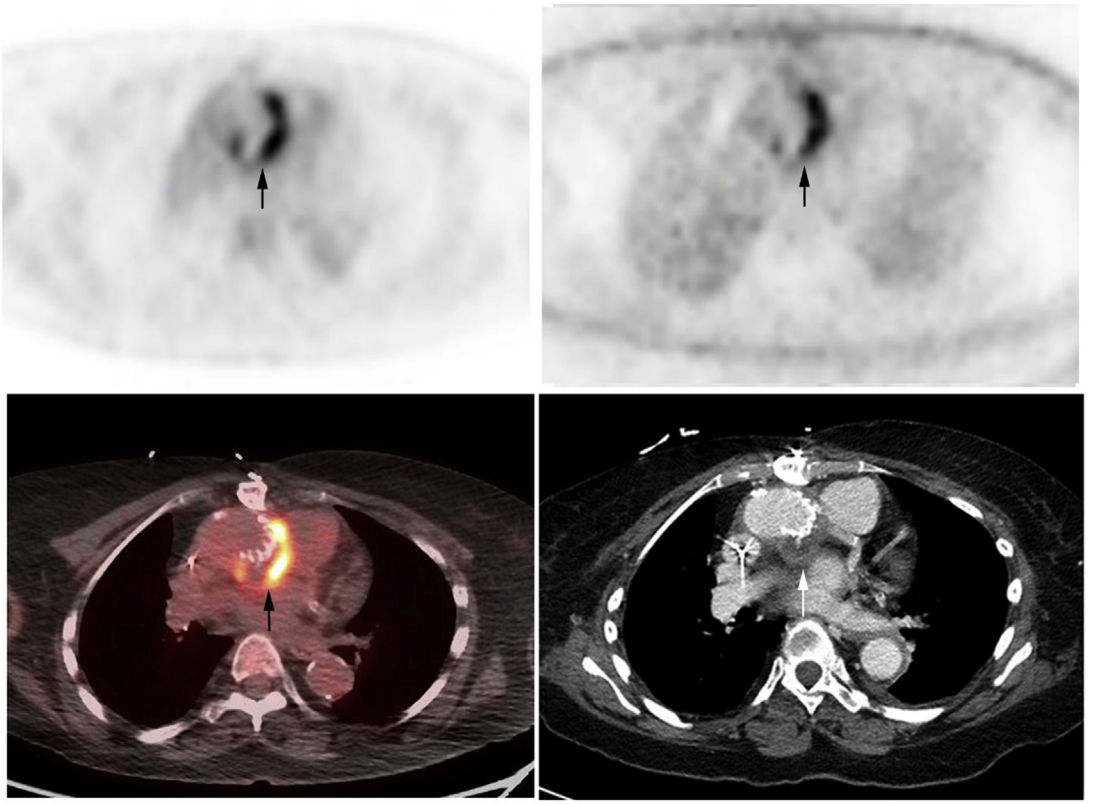

Fig. 12. Attenuation corrected (*top left*), non-attenuation-corrected (*top right*), fused PET/CT (*bottom left*), and CT (bottom right)images demonstrate prominent hypermetabolic activity involving and surrounding the infected transaortic valve prosthesis with a perivalvular fluid collection/abscess (*arrows*) in a patient with methicillin-resistant Staphylococcus aureus bacteremia.

Optimal patient preparation protocols are not well established. A combination of interventions is the norm. These include avoidance of strenuous exercise and a no-carbohydrate to very-low-carbohydrate (<3 g), high-protein, and high-fat diet (>35 g) for at least the day prior to the scan followed by an overnight fast.[11] Glucose-containing intravenous medications or fluids are prohibited. An alternative option (for patients who cannot follow the diet) is fasting for greater than or equal to 18 hours before the study.[41] The role of intravenous unfractionated heparin (induces lipolysis by lipoprotein lipase activation and increases FFA in the blood) is unclear.[41] Heparin (dose 10–50 IU/kg) is given 15 minutes before FDG injection with lower doses increasing FFA without significant partial thromboplastin time prolongation. Approximately 60 minutes after intravenous FDG injection (8–10 mCi [296–370 MBq]), whole-body (typically eyes to thighs) and dedicated cardiac PET/CT or PET/MR images are acquired.

Both CT attenuation-corrected and non–attenuation-corrected images are reviewed to differentiate real from artifactual increased tracer uptake due to high-density metal in devices. Fused PET/CT images provide anatomic localization of tracer. Focal or heterogeneous uptake favors infection, whereas diffuse mild uptake may suggest nonspecific inflammatory changes. The methodology and role of semiquantitative SUV in assessment of cardiac and cardiac device infections is unclear.[67]

Noninfectious inflammatory activity may cause false-positive results, such as early after surgery or from foreign body/granulomatous reaction. Thus, it can be challenging to differentiate noninfectious inflammation from infection on FDG-PET for up to 3 months postintervention.[67] The surgical adhesive used to seal an aortic root graft may produce inflammation resulting in false-positive tracer uptake.[11] Other false positives include active thrombi, soft atherosclerotic plaques, vasculitis, primary cardiac tumors, and metastasis.[63] False-

negative FDG PET (no or low uptake) may be seen in mild infection with a low bacterial load, small vegetations, chronic or indolent infection with slow-growing bacteria, infection with fastidious or biofilm-forming bacteria, and partially treated infection. Abnormal noncardiac FDG uptake may be potential sites of embolic infection (osteomyelitis, intra-abdominal abscess, and so forth). Brain septic emboli identification is limited by high physiologic brain cortical FDG uptake. Compared with alternative leukocyte scintigraphy, FDG PET has the advantage of shorter procedure duration (<2 hours), high sensitivity, and better spatial and contrast resolution but suffers from lower specificity because FDG also can accumulate in noninfectious inflammatory cells.

In conclusion, FDG PET is a promising and emerging adjunctive diagnostic tool that can help in the diagnosis, disease severity assessment, and evaluation of embolic complications and prognosis of potentially life-threatening cardiac and cardiac device infections.

CLINICS CARE POINTS

- PET myocardial perfusion imaging has distinct advantages over SPECT, specifically in patient subgroups including obesity, high risk anatomy (multivessel and left main disease), diabetes and chronic kidney disease.
- PET viability assessment is reasonable in most patients with LV systolic dysfunction and known significant underlying coronary artery disease.
- Patient preparation protocols for assessment of cardiac inflammation with FDG PET involves a combination of fasting, high fat and no to low carbohydrate diet, and avoidance of exercise. Role of intravenous unfractionated heparin is unclear.

REFERENCES

1. Roger VL. Epidemiology of myocardial infarction. Med Clin North Am 2007;91(4):537–52, ix.
2. Mozaffarian D, Benjamin EJ, Go AS, et al. Executive summary: heart disease and stroke statistics–2016 update: a report from the American Heart Association. Circulation 2016;133(4):447–54.
3. Rosamond W, Flegal K, Furie K, et al. Heart disease and stroke statistics–2008 update: a report from the American Heart Association Statistics Committee and Stroke Statistics Subcommittee. Circulation 2008;117(4):e25–146.
4. De Bruyne B, Oldroyd KG, Pijls NHJ. Microvascular (Dys)Function and clinical outcome in stable coronary disease. J Am Coll Cardiol 2016;67(10):1170–2.
5. Bateman TM, Maddahi J, Gray RJ, et al. Diffuse slow washout of myocardial thallium-201: a new scintigraphic indicator of extensive coronary artery disease. J Am Coll Cardiol 1984;4(1):55–64.
6. Gupta A, Taqueti VR, van de Hoef TP, et al. Integrated noninvasive physiological assessment of coronary circulatory function and impact on cardiovascular mortality in patients with stable coronary artery disease. Circulation 2017;136(24):2325–36.
7. Bajaj NS, Bhambhvani P. SPECT-derived absolute myocardial perfusion measures: a step in the right direction. J Nucl Cardiol 2019. https://doi.org/10.1007/s12350-019-01972-w.
8. Bajaj NS, Osborne MT, Gupta A, et al. Coronary microvascular dysfunction and cardiovascular risk in obese patients. J Am Coll Cardiol 2018;72(7):707–17.
9. Murthy VL, Bateman TM, Beanlands RS, et al. Clinical quantification of myocardial blood flow using PET: joint position paper of the SNMMI cardiovascular Council and the ASNC. J Nucl Cardiol 2018;25(1):269–97.
10. Bateman TM, Dilsizian V, Beanlands RS, et al. American Society of Nuclear Cardiology and Society of Nuclear Medicine and molecular imaging joint position statement on the clinical indications for myocardial perfusion PET. J Nucl Cardiol 2016;23(5):1227–31.
11. Dilsizian V, Bacharach SL, Beanlands RS, et al. ASNC imaging guidelines/SNMMI procedure standard for positron emission tomography (PET) nuclear cardiology procedures. J Nucl Cardiol 2016;23(5):1187–226.
12. Cahill TJ, Kharbanda RK. Heart failure after myocardial infarction in the era of primary percutaneous coronary intervention: mechanisms, incidence and identification of patients at risk. World J Cardiol 2017;9(5):407–15.
13. Moran AE, Forouzanfar MH, Roth GA, et al. The global burden of ischemic heart disease in 1990 and 2010: the Global Burden of Disease 2010 study. Circulation 2014;129(14):1493–501.
14. Löffler AI, Kramer CM. Myocardial viability testing to guide coronary revascularization. Interv Cardiol Clin 2018;7(3):355–65.
15. Di Carli MF, Asgarzadie F, Schelbert HR, et al. Quantitative relation between myocardial viability and improvement in heart failure symptoms after

revascularization in patients with ischemic cardiomyopathy. Circulation 1995;92(12):3436–44.
16. Di Carli MF, Maddahi J, Rokhsar S, et al. Long-term survival of patients with coronary artery disease and left ventricular dysfunction: implications for the role of myocardial viability assessment in management decisions. J Thorac Cardiovasc Surg 1998;116(6):997–1004.
17. Sheikine Y, Di Carli MF. Integrated PET/CT in the assessment of etiology and viability in ischemic heart failure. Curr Heart Fail Rep 2008;5(3):136–42.
18. Ling LF, Marwick TH, Flores DR, et al. Identification of therapeutic benefit from revascularization in patients with left ventricular systolic dysfunction: inducible ischemia versus hibernating myocardium. Circ Cardiovasc Imaging 2013;6(3):363–72.
19. D'Egidio G, Nichol G, Williams KA, et al. Increasing benefit from revascularization is associated with increasing amounts of myocardial hibernation: a substudy of the PARR-2 trial. JACC Cardiovasc Imaging 2009;2(9):1060–8.
20. Anavekar NS, Chareonthaitawee P, Narula J, et al. Revascularization in patients with severe left ventricular dysfunction: is the assessment of viability still viable? J Am Coll Cardiol 2016;67(24):2874–87.
21. Allman KC, Shaw LJ, Hachamovitch R, et al. Myocardial viability testing and impact of revascularization on prognosis in patients with coronary artery disease and left ventricular dysfunction: a meta-analysis. J Am Coll Cardiol 2002;39(7):1151–8.
22. Schelbert HR. PET contributions to understanding normal and abnormal cardiac perfusion and metabolism. Ann Biomed Eng 2000;28(8):922–9.
23. Beanlands RS, Nichol G, Huszti E, et al. F-18-fluorodeoxyglucose positron emission tomography imaging-assisted management of patients with severe left ventricular dysfunction and suspected coronary disease: a randomized, controlled trial (PARR-2). J Am Coll Cardiol 2007;50(20):2002–12.
24. Mc Ardle B, Shukla T, Nichol G, et al. Long-term follow-up of outcomes with f-18-fluorodeoxyglucose positron emission tomography imaging-assisted management of patients with severe left ventricular dysfunction secondary to coronary disease. Circ Cardiovasc Imaging 2016;9(9):e004331.
25. Abraham A, Nichol G, Williams KA, et al. 18F-FDG PET imaging of myocardial viability in an experienced center with access to 18F-FDG and integration with clinical management teams: the Ottawa-FIVE substudy of the PARR 2 trial. J Nucl Med 2010;51(4):567–74.
26. O'Meara E, Mielniczuk LM, Wells GA, et al. Alternative Imaging Modalities in Ischemic Heart Failure (AIMI-HF) IMAGE HF Project I-A: study protocol for a randomized controlled trial. Trials 2013;14:218.
27. Yancy CW, Jessup M, Bozkurt B, et al. 2017 ACC/AHA/HFSA focused update of the 2013 ACCF/AHA guideline for the management of heart failure: a report of the American College of Cardiology/American Heart Association Task Force on Clinical Practice Guidelines and the Heart Failure Society of America. Circulation 2017;136(6):e137–61.
28. Patel MR, White RD, Abbara S, et al. 2013 ACCF/ACR/ASE/ASNC/SCCT/SCMR appropriate utilization of cardiovascular imaging in heart failure: a joint report of the American College of Radiology Appropriateness Criteria Committee and the American College of Cardiology Foundation Appropriate Use Criteria Task Force. J Am Coll Cardiol 2013;61(21):2207–31.
29. Garcia MJ, Kwong RY, Scherrer-Crosbie M, et al. State of the art: imaging for myocardial viability: a scientific statement from the American Heart Association. Circ Cardiovasc Imaging 2020;13(7):e000053.
30. Baughman RP, Lower EE, du Bois RM. Sarcoidosis. Lancet 2003;361(9363):1111–8.
31. Llanos O, Hamzeh N. Sarcoidosis. Med Clin North Am 2019;103(3):527–34.
32. Statement on sarcoidosis. Joint Statement of the American Thoracic Society (ATS), the European Respiratory Society (ERS) and the World Association of Sarcoidosis and Other Granulomatous Disorders (WASOG) adopted by the ATS Board of Directors and by the ERS Executive Committee, February 1999. Am J Respir Crit Care Med 1999;160(2):736–55.
33. Vignaux O. Cardiac sarcoidosis: spectrum of MRI features. AJR Am J Roentgenol 2005;184(1):249–54.
34. Kim JS, Judson MA, Donnino R, et al. Cardiac sarcoidosis. Am Heart J 2009;157(1):9–21.
35. Schatka I, Bengel FM. Advanced imaging of cardiac sarcoidosis. J Nucl Med 2014;55(1):99–106.
36. Perez IE, Garcia MJ, Taub CC. Multimodality imaging in cardiac sarcoidosis: is there a winner? Curr Cardiol Rev 2016;12(1):3–11.
37. Cooper LT, Baughman KL, Feldman AM, et al. The role of endomyocardial biopsy in the management of cardiovascular disease: a scientific statement from the American Heart Association, the American College of Cardiology, and the European Society of Cardiology Endorsed by the Heart Failure Society of America and the Heart Failure Association of the European Society of Cardiology. Eur Heart J 2007;28(24):3076–93.
38. Okada DR, Bravo PE, Vita T, et al. Isolated cardiac sarcoidosis: a focused review of an under-recognized entity. J Nucl Cardiol 2018;25(4):1136–46.
39. Birnie DH, Sauer WH, Bogun F, et al. HRS expert consensus statement on the diagnosis and

management of arrhythmias associated with cardiac sarcoidosis. Heart Rhythm 2014;11(7):1305–23.
40. Kumita S, Yoshinaga K, Miyagawa M, et al. Recommendations for (18)F-fluorodeoxyglucose positron emission tomography imaging for diagnosis of cardiac sarcoidosis-2018 update: Japanese Society of Nuclear Cardiology recommendations. J Nucl Cardiol 2019;26(4):1414–33.
41. Chareonthaitawee P, Beanlands RS, Chen W, et al. Joint SNMMI-ASNC expert consensus document on the Role of (18)F-FDG PET/CT in cardiac sarcoid detection and therapy monitoring. J Nucl Med 2017; 58(8):1341–53.
42. Bois JP, Muser D, Chareonthaitawee P. PET/CT evaluation of cardiac sarcoidosis. PET Clin 2019;14(2): 223–32.
43. Osborne MT, Hulten EA, Murthy VL, et al. Patient preparation for cardiac fluorine-18 fluorodeoxyglucose positron emission tomography imaging of inflammation. J Nucl Cardiol 2017;24(1):86–99.
44. Tilkemeier PL, Wackers FJ. Myocardial perfusion planar imaging. J Nucl Cardiol 2006;13(6):e91–6.
45. Skali H, Schulman AR, Dorbala S. 18F-FDG PET/CT for the assessment of myocardial sarcoidosis. Curr Cardiol Rep 2013;15(4):352.
46. Blankstein R, Osborne M, Naya M, et al. Cardiac positron emission tomography enhances prognostic assessments of patients with suspected cardiac sarcoidosis. J Am Coll Cardiol 2014;63(4):329–36.
47. Vachatimanont S, Kunawudhi A, Promteangtrong C, et al. Benefits of [(68)Ga]-DOTATATE PET-CT comparable to [(18)F]-FDG in patient with suspected cardiac sarcoidosis. J Nucl Cardiol 2020.
48. White JA, Rajchl M, Butler J, et al. Active cardiac sarcoidosis: first clinical experience of simultaneous positron emission tomography–magnetic resonance imaging for the diagnosis of cardiac disease. Circulation 2013;127(22):e639–41.
49. Wicks EC, Menezes LJ, Barnes A, et al. Diagnostic accuracy and prognostic value of simultaneous hybrid 18F-fluorodeoxyglucose positron emission tomography/magnetic resonance imaging in cardiac sarcoidosis. Eur Heart J Cardiovasc Imaging 2018; 19(7):757–67.
50. Bargout R, Kelly RF. Sarcoid heart disease: clinical course and treatment. Int J Cardiol 2004;97(2):173–82.
51. Schuller JL, Zipse M, Crawford T, et al. Implantable cardioverter defibrillator therapy in patients with cardiac sarcoidosis. J Cardiovasc Electrophysiol 2012; 23(9):925–9.
52. Epstein AE, Dimarco JP, Ellenbogen KA, et al. ACC/AHA/HRS 2008 guidelines for device-based therapy of cardiac rhythm abnormalities: executive summary. Heart Rhythm 2008;5(6):934–55.
53. Lower EE, Baughman RP. The use of low dose methotrexate in refractory sarcoidosis. Am J Med Sci 1990;299(3):153–7.
54. Rosenthal DG, Anderson ME, Petek BJ, et al. Invasive hemodynamics and rejection rates in patients with cardiac sarcoidosis after heart transplantation. Can J Cardiol 2018;34(8):978–82.
55. Prutkin JM, Reynolds MR, Bao H, et al. Rates of and factors associated with infection in 200 909 Medicare implantable cardioverter-defibrillator implants: results from the National Cardiovascular Data Registry. Circulation 2014;130(13):1037–43.
56. Orvin K, Goldberg E, Bernstine H, et al. The role of FDG-PET/CT imaging in early detection of extracardiac complications of infective endocarditis. Clin Microbiol Infect 2015;21(1):69–76.
57. Juneau D, Golfam M, Hazra S, et al. Molecular Imaging for the diagnosis of infective endocarditis: a systematic literature review and meta-analysis. Int J Cardiol 2018;253:183–8.
58. Mahmood M, Kendi AT, Ajmal S, et al. Meta-analysis of 18F-FDG PET/CT in the diagnosis of infective endocarditis. J Nucl Cardiol 2019;26(3):922–35.
59. Mahmood M, Kendi AT, Farid S, et al. Role of (18)F-FDG PET/CT in the diagnosis of cardiovascular implantable electronic device infections: a meta-analysis. J Nucl Cardiol 2019;26(3):958–70.
60. Tam MC, Patel VN, Weinberg RL, et al. Diagnostic accuracy of FDG PET/CT in suspected LVAD infections: a case series, systematic review, and meta-analysis. JACC Cardiovasc Imaging 2020;13(5): 1191–202.
61. San S, Ravis E, Tessonier L, et al. Prognostic value of (18)F-fluorodeoxyglucose positron emission tomography/computed tomography in infective endocarditis. J Am Coll Cardiol 2019;74(8):1031–40.
62. Diemberger I, Bonfiglioli R, Martignani C, et al. Contribution of PET imaging to mortality risk stratification in candidates to lead extraction for pacemaker or defibrillator infection: a prospective single center study. Eur J Nucl Med Mol Imaging 2019; 46(1):194–205.
63. Habib G, Lancellotti P, Antunes MJ, et al. 2015 ESC Guidelines for the management of infective endocarditis: The Task Force for the Management of Infective Endocarditis of the European Society of Cardiology (ESC). Endorsed by: European Association for Cardio-Thoracic Surgery (EACTS), the European Association of Nuclear Medicine (EANM). Eur Heart J 2015;36(44):3075–128.
64. Blomstrom-Lundqvist C, Traykov V, Erba PA, et al. European Heart Rhythm Association (EHRA) international consensus document on how to prevent, diagnose, and treat cardiac implantable electronic device infections-endorsed by the Heart Rhythm Society (HRS), the Asia Pacific Heart Rhythm Society (APHRS), the Latin American Heart Rhythm Society (LAHRS), International Society for Cardiovascular Infectious Diseases (ISCVID), and the European Society of Clinical

Microbiology and Infectious Diseases (ESCMID) in collaboration with the European Association for Cardio-Thoracic Surgery (EACTS). Eur Heart J 2020;41(21):2012–32.

65. Mochizuki T, Tsukamoto E, Kuge Y, et al. FDG uptake and glucose transporter subtype expressions in experimental tumor and inflammation models. J Nucl Med 2001;42(10):1551–5.

66. Bhambhvani P. Challenges of cardiac inflammation imaging with F-18 FDG positron emission tomography. J Nucl Cardiol 2017;24(1):100–2.

67. Mahmood M, Abu Saleh O. The role of 18-F FDG PET/CT in imaging of endocarditis and cardiac device infections. Semin Nucl Med 2020;50(4):319–30.